Self-organization and properties of dilute aqueous solutions of cetyltrimethylammonium bromide in a range of physiologically important temperatures*

I. S. Ryzhkina, Yu. V. Kiseleva, O. A. Mishina, L. I. Murtazina, A. I. Litvinov, M. K. Kadirov, and A. I. Konovalov*

A. E. Arbuzov Institute of Organic and Physical Chemistry, Kazan Scientific Center of the Russian Academy of Sciences, 8 ul. Akad. Arbuzova, 420088 Kazan, Russian Federation.
Fax: +7 (843) 273 1872. E-mail: ryzhkina@iopc.ru

A combination of physicochemical methods (dynamic light scattering, nanoparticle tracking analysis, conductometry, tensiometry, and ESR spectroscopy) revealed that dilute solutions ($1 \cdot 10^{-3}$, $1.0 \cdot 10^{-4}$, $1.0 \cdot 10^{-7}$, and $1.0 \cdot 10^{-9}$ mol L^{-1}) of surfactant (cetyltrimethylammonium bromide) in a temperature range of 25—45 °C are self-organized dispersed systems. As the temperature increases, the systems undergo rearrangements specific for each studied concentration, which is reflected as nonmonotonic temperature dependences of the parameters of domains ($1 \cdot 10^{-3}$ and $1.0 \cdot 10^{-4}$ mol L^{-1}) and nanoassociates ($1.0 \cdot 10^{-7}$ and $1.0 \cdot 10^{-9}$ mol L^{-1}) and also as interrelated dependences of the conductivity of solutions with extremes at 30, 37, and 40 °C. The ESR experiments show a nonmonotonic decrease in the rotational diffusion correlation time (τ_{cor}) of 2,2,6,6-tetramethylpiperidine-1-oxyl (TEMPO) in the temperature dependences of τ_{cor} with the temperature increase from 25 to 45 °C and the appearance of two to three plateaus, one of which (in a range of 36—40 °C) is observed in the temperature dependences for all studied concentrations.

Key words: cetyltrimethylammonium bromide, dilute solutions, temperature, self-organization, nanoassociates, domains, particle size, conductivity, ESR spectroscopy, 2,2,6,6-tetramethylpiperidine-1-oxyl.

Among unsolved problems of the theory of aqueous solutions are anomalous temperature dependences of their physicochemical properties and spectral characteristics.[1—8] It was shown recently[9,10] that nonmonotonic temperature and concentration dependences of the physicochemical properties of solutions can be explained by rearrangements of nanostructures formed in solutions, whose size lies in a range of hundreds of nanometers and which are similar to supramolecular domains[11—14] found in aqueous solutions of organic and inorganic substances in the concentration range from $1 \cdot 10^{-6}$ to 6 mol L^{-1}.

It has recently been found that highly dilute (10^{-6}—10^{-20} mol L^{-1}) aqueous solutions of many biologically active substances at 25 °C are self-organized dispersed systems. In these dispersed systems under some conditions, the most important of which are the structure of the solute and external physical fields, nanosized ensembles (nanoassociates) (100—400 nm) are formed, and their rearrangement results in nonmonotonic concentration dependences of the physicochemical and, probably, biological properties of highly dilute solutions (see review[15] and references cited therein). The temperature dependences of the parameters of nanoassociates and properties of highly dilute solutions were not studied to date.

Solutions of surfactant cetyltrimethylammonium bromide (CTAB) are convenient and informative model systems for studying the temperature influence on self-organization and physicochemical properties of dilute solutions. Solutions of CTAB have been long ago and widely used in basic research and industrial technologies as detergents, antibacterial drugs, micellar catalysts, modifiers of water-soluble polymer of synthetic and natural origin, *etc.*[16—27] However, before our works[15,28,29] only the properties of individual and mixed solutions containing CTAB in micellar (above the critical micelle concentration, $8.0 \cdot 10^{-4}$ mol L^{-1}) or premicellar[30,31] ($1 \cdot 10^{-5}$—$1 \cdot 10^{-4}$ mol L^{-1}) concentrations were studied.

The study of CTAB solutions using an original procedure involving the storage of solutions under natural conditions and at a decreased level of external physical fields showed[15,29] that nanoassociates ($1.0 \cdot 10^{-6}$—$1.0 \cdot 10^{-12}$ mol L^{-1}), domains ($1 \cdot 10^{-2}$—$1.0 \cdot 10^{-5}$ mol L^{-1}), and micelles (above $8.0 \cdot 10^{-4}$ mol L^{-1}) are formed at 25 °C in CTAB solutions in a wide concentration range ($1 \cdot 10^{-2}$—$1.0 \cdot 10^{-12}$ mol L^{-1}). Concentration rearrangements of

* Dedicated to Academician of the Russian Academy of Sciences V. I. Minkin on the occasion of his 80th birthday.

Published in Russian in *Izvestiya Akademii Nauk. Seriya Khimicheskaya,* No. 3, pp. 0579—0589, March, 2015.

nanoassociates and domains accompanied by a change in their size and ζ potential result in the nonmonotonic character of the dependences of the conductivity, pH, and dielectric constant of dilute solutions ($1.0 \cdot 10^{-4}$—$1.0 \cdot 10^{-12}$ mol L^{-1}), the appearance of the absorbance (in the concentration range $3.0 \cdot 10^{-7}$—$3.0 \cdot 10^{-8}$ mol L^{-1}), and the stimulating effect on the bacteria growth (in the concentration range $1.0 \cdot 10^{-9}$—$1.0 \cdot 10^{-11}$ mol L^{-1}).[15,29]

The purpose of this work is to study the influence of physiologically important temperatures (25—45 °C) on the self-organization and properties of dilute solutions of CTAB with concentrations of $1 \cdot 10^{-3}$, $1.0 \cdot 10^{-4}$, $1.0 \cdot 10^{-7}$, and $1.0 \cdot 10^{-9}$ mol L^{-1} by dynamic light scattering (DLS), nanoparticle tracking analysis (NTA), conductometry, tensiometry, pH-metry, and spin probe ESR spectroscopy.

Experimental

Solutions of CTAB (Sigma-Aldrich, USA) were prepared and studied under the usual conditions using freshly prepared bidistilled water, whose conductivity did not exceed 1.5 μS cm^{-1}. Solutions were prepared by the method of consecutive decimal dilutions from the stock solution of the substance with a concentration of $1 \cdot 10^{-2}$ mol L^{-1} as described.[15,29] The solutions were stirred with an IKA lab dancer minishaker. The conductivity (χ), surface tension (σ), and pH of solutions were measured on an inoLab Cond Level 1 conductometer (EcoInstrument), a Sigma 720 ET tensiometer (KSV Instruments), and an inoLab pH 720 pH-meter (EcoInstrument) under temperature-controlled conditions. The relative measurement error for χ did not exceed 10%, and that for pH was 1.5%. The temperature effect on the physicochemical properties of solutions were studied at 25, 30, 35, 37, 40, and 45 °C with a Termeks thermostat (OOO Termeks, Tomsk, Russia). The controlled temperature ranged from +15 to +201 °C. Prior to measurement, the working solutions were kept for 5—7 h under temperature-controlled conditions.

The size (effective hydrodynamic diameter of kinetically mobile particles at the maximum of the distribution curve, *D*) and the ζ potential of the particles were determined by the dynamic light scattering (DLS) method on a Zetasizer Nano ZS high-sensitivity analyzer (Malvern Instruments). The relative measurement error for the size and ζ potential did not exceed 15%.

Solutions of CTAB were studied by the NTA method on a Nanosight LM 10 analyzer (NanoSight, Great Britain) in the HS-BF configuration for visualization of particles and measurement of their hydrodynamic size and concentration. The NTA method is based on the observation of Brownian motion of individual nanoparticles by the irradiation of the sample with a focused laser beam. Nanoparticles behave as point scatterers and look like light spots against the dark background. A high-sensitivity camera recorded Brownian motion of centers of these spots. Videotape recording in the real time is transmitted to a personal computer for processing: isolation of individual nanoparticles on each frame and tracking particle motions between frames. The velocity of Brownian motion expressed as a root-mean-square shift of the particle per certain time is related to the particle size by the Stokes—Einstein equation. The second measured parameter is the concentration of each fraction of nanoparticles. The NTA method can be applied to particles with the size from 10 nm to 1 μm at the particle concentration from 10^7 to 10^9 in 1 mL of the solution. The method is absolute and does not require calibration. The used Nanosight LM10 HS-BF instrument is equipped with a laser source with a wavelength of 405 nm and a power of 65 mW and a high-sensitivity EMCCD Andor Luca scientific camera. The measurements were carried out according to recommendations of the ASTM E2834-12 standard.[32] Videotapes of Brownian motion were processed using the NTA 2.3 software (Nanosight, Great Britain). Solutions were filtered through filters with a pore diameter of 0.45 μm (Iso-Disc N-25-4 Nylon, 25 mm×0.45 μm, Supelco, USA).

ESR spectra were recorded on an Elexsys E500 Bruker X-range ESR spectrometer. The studied solutions were placed in a cylindrical ampule with an internal diameter of 1 mm and multiply purged with nitrogen. Classical spin probe 2,2,6,6-tetramethylpiperidine-1-oxyl (TEMPO) (Sigma) was used. The ESR spectra of samples were recorded in the *Rapid-scan* mode during the whole irradiation time. All ESR experiments using the spin probe were carried out three times. The relative experimental error was ~20%. The temperature of the sample was maintained during the experiment from 299 to 318 K with an increment of 1°.

Results and Discussion

The particle size distribution at 25, 37, and 45 °C in CTAB solutions with the concentrations $1 \cdot 10^{-3}$, $1.0 \cdot 10^{-4}$, $1.0 \cdot 10^{-7}$, and $1 \cdot 10^{-9}$ mol L^{-1} is presented in Fig. 1. As can be seen from the data in Fig. 1, *a* at 25 °C, micelles with a size of 4 nm and structures, whose size is several hundreds nm, are formed in a solutions with the CTAB concentration equal to $1 \cdot 10^{-3}$ mol L^{-1}. In the concentration range from $1.0 \cdot 10^{-4}$ to $1.0 \cdot 10^{-9}$ mol L^{-1}, the solution contains only structures with a size of hundreds nm (see Fig. 1, *d*, *g*, *j*).

No particles were observed in CTAB solutions with concentrations of $1.0 \cdot 10^{-6}$—$1.0 \cdot 10^{-12}$ mol L^{-1} stored in a permalloy container, *i.e.*, a concentration of $1.0 \cdot 10^{-5}$ mol L^{-1} is threshold.[15,29] This means that the structures with a size of hundreds nm that are formed and stored under natural conditions in solutions with the concentrations lower than the threshold one ($1.0 \cdot 10^{-6}$—$1.0 \cdot 10^{-12}$ mol L^{-1}) are nanoassociates, while those formed in solutions with concentrations of $1.0 \cdot 10^{-4}$—$1.0 \cdot 10^{-5}$ mol L^{-1} are domains (see Fig. 1, *d*, *g*, *j*).

An analysis of the concentration dependences of the sizes and ζ potential of supramolecular domains and nanoassociates, as well as those of the conductivity (Fig. 2), absorbance, and dielectric constant,[29] which were obtained at 25 °C, revealed that the extreme changes in the parameters of the domains and nanoassociates and the physicochemical properties of the solutions are observed also for solutions with concentrations of $1 \cdot 10^{-3}$, $1.0 \cdot 10^{-4}$, $1.0 \cdot 10^{-7}$, and $1.0 \cdot 10^{-9}$ mol L^{-1}. We chose just these concentrations for studying the temperature influence on the parameters of the domains and nanoassociates and on the properties of solutions.

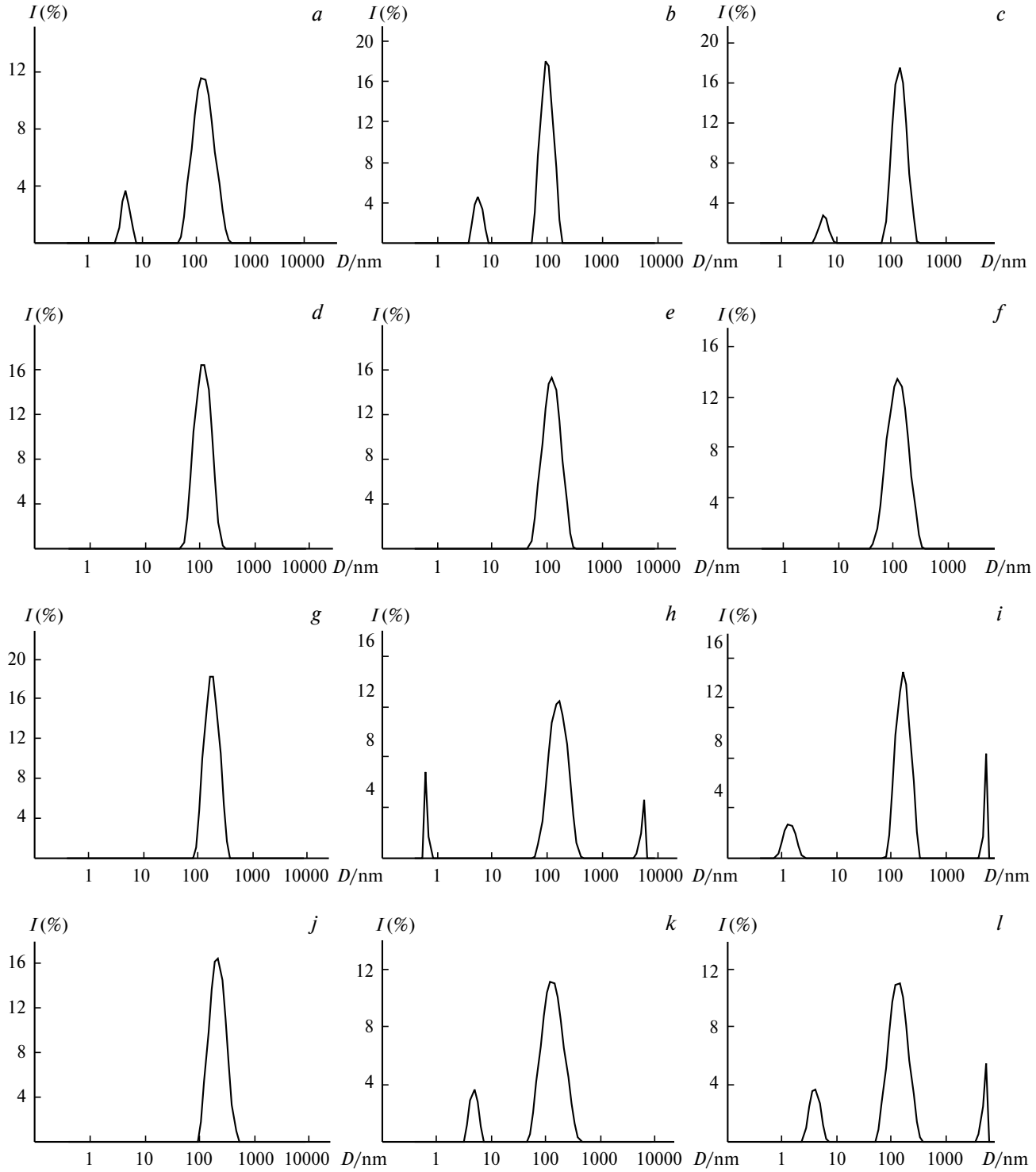

Fig. 1. Particle size distribution in aqueous solutions of CTAB with the concentrations $1 \cdot 10^{-3}$ (*a*, *b*, *c*), $1.0 \cdot 10^{-4}$ (*d*, *e*, *f*), $1.0 \cdot 10^{-7}$ (*g*, *h*, *i*), and $1.0 \cdot 10^{-9}$ mol L^{-1} (*j*, *k*, *l*), which were kept under temperature-controlled conditions at 25 (*a*, *d*, *g*, *j*), 37 (*b*, *e*, *h*, *k*), and 45 °C (*c*, *f*, *i*, *l*). *D* is the particle size, and *I* is the scattered light intensity.

We used the method of nanoparticle tracking analysis to confirm the sizes of the domains and nanoassociates determined by the DLS method at 25 °C and the fact that the number of these nanoparticles in dilute solutions of CTAB is fairly high. In the CTAB concentration range from $1 \cdot 10^{-2}$ to $1.0 \cdot 10^{-4}$ mol L^{-1}, the particles are visualized in solution, whose size was tens and hundreds of nanometers and the number of these structures exceeds 10^{10}

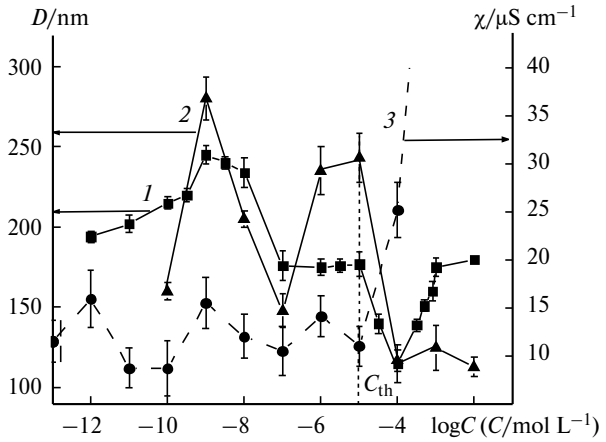

Fig. 2. Particle size (*D*) (*1*, *2*) and conductivity (χ) (*3*) of a CTAB solution *vs* concentration at 25 (*1*, *3*) and 40 °C (*2*). C_{th} is the threshold concentration.

particles in 1 mL. Although the NTA method at the particle concentration exceeding 10^{10} particles in 1 mL does not allow one to exactly determine the size and number of formed structures, it reliably confirms the formation of particles, whose average size is estimated as hundreds nm, in this range of CTAB concentrations. The image obtained by the study of a CTAB solution with a concentration of $1 \cdot 10^{-3}$ mol L^{-1} is presented in Fig. 3, *a*.

The same number of particles, $3 \cdot 10^8$ in 1 mL of the solution (Fig. 3, *b*), is detected in CTAB solutions with the concentrations $1.0 \cdot 10^{-5}$ and $1.0 \cdot 10^{-7}$ mol L^{-1}. The particle size ranges from 40 to 300 nm, and the average hydrodynamic radius is approximately 120 nm. The established values of the particle number and size in solutions with concentrations of $1.0 \cdot 10^{-5}$ and $1.0 \cdot 10^{-7}$ mol L^{-1} are optimum for the NTA analysis and reliable statistics over the number and size of nanoparticles.

The results obtained by the NTA method are well consistent with the DLS data, according to which supramolecular domains and nanoassociates with the size from 60 to 400 nm and the average diameter about 170 nm, which remains almost unchanged in this concentration range (see Fig. 1, *a*, *d*, *g*, *j* and Fig. 2), are detected in CTAB solutions with concentrations of $1.0 \cdot 10^{-5}$—$1.0 \cdot 10^{-7}$ mol L^{-1}. No particles were found in freshly prepared bidistilled water.

Similar results were obtained in Ref. 9 and showed that the number of particles formed in a solution of tyrosine phosphate in a concentration range of $1 \cdot 10^{-4}$—$3 \cdot 10^{-3}$ mol L^{-1} at 25 °C lies in the range from $1 \cdot 10^8$ to $1 \cdot 10^7$ particles in 1 mL, and the average particle diameter in the whole range is 160 nm. There also data[9] that the particle number in purified water can be 10^6 in 1 mL, *i.e.*, by two orders of magnitude lower than that in the studied solutions of tyrosine phosphate.

Thus, the NTA method gave an additional confirmation of the formation of domains with a size of hundreds

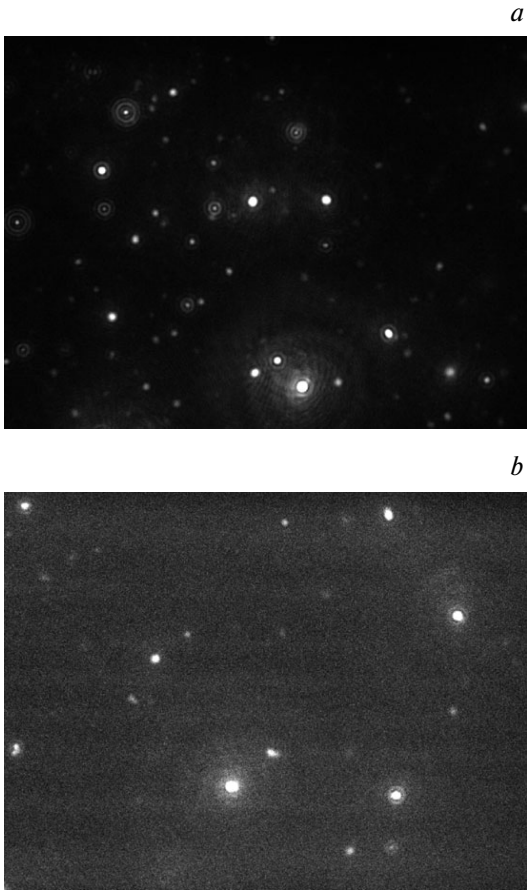

Fig. 3. Images of CTAB solutions obtained by the NTA method at CTAB concentrations equal to $1 \cdot 10^{-3}$ mol L^{-1} (*a*) (camera level 12) and $1.0 \cdot 10^{-7}$ mol L^{-1} (*b*) (camera level 16), 25 °C.

nm in CTAB solutions with the concentrations $1 \cdot 10^{-2}$—$1 \cdot 10^{-3}$ mol L^{-1}. It was found that the decrease in the CTAB concentration by two orders of magnitude from $1.0 \cdot 10^{-5}$ to $1.0 \cdot 10^{-7}$ mol L^{-1} exerts no effect on the number of domains and nanoassociates, which is $3 \cdot 10^8$ in 1 mL. The obtained result possibly indicates that the domains formed in the range of threshold concentration equal to $1.0 \cdot 10^{-5}$ mol L^{-1} and the more so nanoassociates are mainly formed by quasi-crystalline structures of water.[33]

The particle size distributions obtained by the DLS method for CTAB solutions with concentrations of $1 \cdot 10^{-3}$ and $1.0 \cdot 10^{-4}$ mol L^{-1} in the temperature range 30—45 °C are nearly completely similar to the results obtained at 25 °C. Solutions with concentrations of $1 \cdot 10^{-3}$ mol L^{-1} in the studied temperature range (25—45 °C) exhibit the formation of micelles with the size about 4 nm and supramolecular domains of hundreds nm, whereas only supramolecular domains are formed at $1.0 \cdot 10^{-4}$ mol L^{-1} (see Fig. 1).

Unlike 25 °C, at 30—45 °C the polymodal particle size distribution was observed in CTAB solutions with concentrations of $1.0 \cdot 10^{-7}$ and $1.0 \cdot 10^{-9}$ mol L^{-1} (see Fig. 1,

b, *e*, *h*, *k* (37 °C) and *c*, *f*, *i*, *l* (45 °C)). However, the structures of hundreds nm, being nanoassociates, predominate in light scattering intensity with a content of 70—80%.

The temperature dependences of the sizes of the structures prevailing in intensity are presented in Fig. 4. As can be seen, the sizes of the domains and nanoassociates formed in solutions with the CTAB concentrations equal to $1 \cdot 10^{-3}$, $1.0 \cdot 10^{-4}$, and $1.0 \cdot 10^{-9}$ mol L^{-1} (see Fig. 4, curves *1*, *2*, and *4*) change with temperature nonmonotonically and specifically for each concentration with extreme values about 30, 37, and 40 °C. A solution of CTAB with a concentration of $1.0 \cdot 10^{-7}$ mol L^{-1} exhibits an insignificant smooth decrease in the nanoassociate size with the temperature increase to 40 °C, and the sizes of the associates remain unchanged when this temperature is exceeded (see Fig. 4, curve *3*).

In a CTAB solution with a concentration of $1 \cdot 10^{-3}$ mol L^{-1}, the temperature increase from 30 to 37 °C is accompanied by a twofold decrease in the domain size from 170 to 80 nm, and then in the temperature range 37—45 °C their size again increases and becomes approximately equal to the value determined at 30 °C (Fig. 4, curve *1*). The run of the temperature dependence of the domain size at the CTAB concentration equal to $1 \cdot 10^{-3}$ mol L^{-1} is similar to the run of the temperature dependence of the size of CTAB micelles.[16] This is probably explained by the fact that at the temperature higher than the Krafft point (26 °C) the solubility of CTAB enhances, resulting in the shift of the equilibrium toward increasing the number of non-aggregated ions and molecules and, correspondingly, decreasing the size of micelles and domains formed in the range of fairly high CTAB concentrations.

The temperature increase slightly affects the domain size with a decrease in the concentration in the solutions

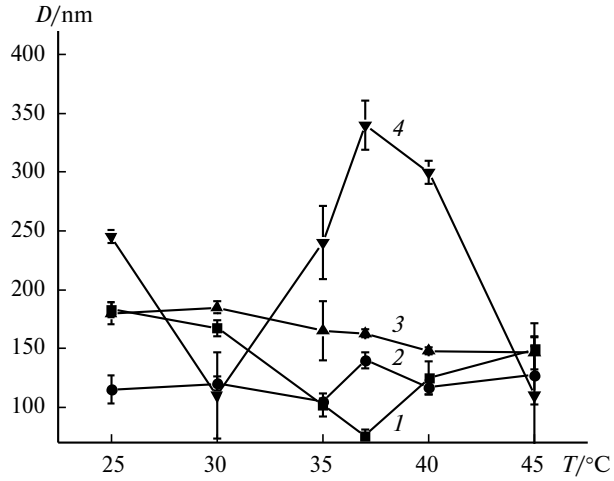

Fig. 4. Temperature dependences of the particle size (*D*) for CTAB solutions with the concentrations $1 \cdot 10^{-3}$ (*1*), $1.0 \cdot 10^{-4}$ (*2*), $1.0 \cdot 10^{-7}$ (*3*), and $1.0 \cdot 10^{-9}$ mol L^{-1} (*4*).

to $1.0 \cdot 10^{-4}$ mol L^{-1}. Only in the temperature range 30—40 °C, a minor increase in the domain size is first observed from 110 to 150 nm and then their sizes decrease showing an extreme at 37 °C (see Fig. 4, curve *2*).

A more pronounced and complicated shape of the temperature dependence of the nanoassociate size with a minimum at 30 °C (100 nm) and a maximum at 37 °C (350 nm) was obtained for CTAB solutions with a concentration of $1.0 \cdot 10^{-9}$ mol L^{-1} (see Fig. 4, curve *4*). The extreme values of the nanoassociate size and physicochemical properties of the solution are observed at 25 °C just for this concentration[15,29] (see Fig. 2).

Thus, the run of the temperature dependences of the sizes of domains formed at a fairly high concentration of CTAB ($1 \cdot 10^{-3}$ mol L^{-1}) and domains and nanoassociates formed in the ranges of low concentrations ($1.0 \cdot 10^{-4}$ and $1.0 \cdot 10^{-9}$ mol L^{-1}) is opposite and has an extreme at 37 °C (see Fig. 4, curves *1* and *2*, *4*). Probably, this can be explained by different natures of domains formed in the micellar concentration range and in dilute solutions. The dilution of the solution results in a sharp decrease in the number of CTAB cations in the composition of domains and nanoassociates and in an increase in the fraction of structured water, which is especially valid for nanoassociates formed in the range of low concentrations only in the presence of external physical fields.

Figure 2 (curves *1* and *2*) shows the concentration dependences of the size of domains and nanoassociates at 25 and 40 °C. In spite of the fact that the particle distribution in solutions at 25 °C in almost the whole concentration range ($1.0 \cdot 10^{-4}$—$1.0 \cdot 10^{-9}$ mol L^{-1}) is monomodal (see Fig. 1) and in the temperature range 30—45 °C monomodality is retained only at a concentration of $1.0 \cdot 10^{-4}$ mol L^{-1} (see Fig. 1, *e*, *f*), the run of the concentration dependences for the particles with a size of hundreds nm at both temperatures is similar and has extremes at $1 \cdot 10^{-3}$, $1.0 \cdot 10^{-4}$, $1.0 \cdot 10^{-7}$, and $1.0 \cdot 10^{-9}$ mol L^{-1}. The observed symbate character of the concentration dependences of the nanoassociate sizes at 25 and 40 °C confirms and explains the tight interrelation observed earlier for the concentration dependences of the parameters of the nanoassociates at 25 °C and bioeffects of highly dilute solutions of biologically active substances at 35—45 °C.[15,29] In particular, an interrelation was observed[29] between the concentration dependences of the nanoassociate size at 25 °C and the dependence of the growth of bacteria incubated at 37 °C in a nutrient medium with the addition of CTAB solutions of low concentrations.

Let us monitor the influence of the temperature on the ζ potential of particles formed in CTAB solutions with concentrations of $1 \cdot 10^{-3}$, $1.0 \cdot 10^{-4}$, $1.0 \cdot 10^{-7}$, and $1.0 \cdot 10^{-9}$ mol L^{-1} (Fig. 5). The temperature dependences of the ζ potential of the domains and nanoassociates (see Fig. 5) at these concentrations and the dependences of

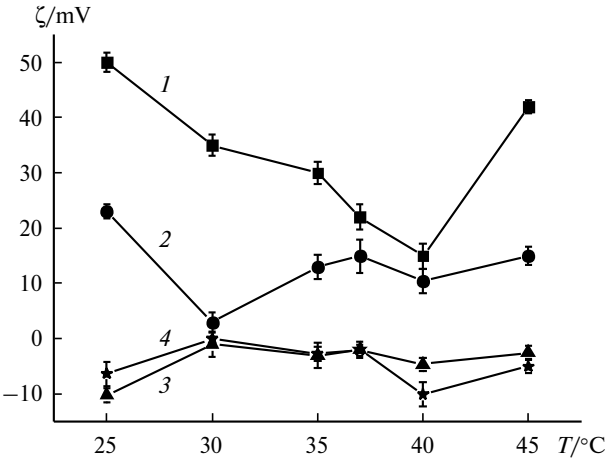

Fig. 5. Temperature dependences of the ζ potential of the particles formed in CTAB solutions with the concentrations $1 \cdot 10^{-3}$ (*1*), $1.0 \cdot 10^{-4}$ (*2*), $1.0 \cdot 10^{-7}$ (*3*), and $1.0 \cdot 10^{-9}$ mol L^{-1} (*4*).

their size (see Fig. 4) change nonmonotonically with extremes at 30, 37, and 40 °C. At a CTAB concentration of $1 \cdot 10^{-3}$ mol L^{-1}, both the size and ζ potential of the domain decrease with temperature and then increase, and the extreme in the temperature dependence of the ζ potential shifts compared to the temperature dependence of the particle size from 37 to 40 °C (see Fig. 5, curve *1*). A more complicated temperature dependence of the ζ potential with three extremes at 30, 37, and 40 °C is observed for a solution with a concentration of $1.0 \cdot 10^{-4}$ mol L^{-1} (see Fig. 5, curve *2*). The run of the dependences of the ζ potentials of nanoassociates formed in solutions with concentrations of $1.0 \cdot 10^{-7}$ and $1.0 \cdot 10^{-9}$ mol L^{-1} in which extremes at 30 and 40 °C are observed (see Fig. 5, curves *3* and *4*) is almost similar. However, at 40 °C the values of ζ potential of nanoassociates formed at $1.0 \cdot 10^{-9}$ mol L^{-1} are twofold higher than those of ζ potential of nanoassociates in solutions with a concentration of $1.0 \cdot 10^{-7}$ mol L^{-1}. As in the case of domains formed in a CTAB solution with a concentration of $1 \cdot 10^{-3}$ mol L^{-1} (see Figs 4 and 5, curves *1*), the position of the extreme of the temperature dependence of the ζ potential of nanoassociates in a solution with the concentration $1.0 \cdot 10^{-9}$ mol L^{-1} shifts compared to the position of the extreme in the temperature dependence of the particle size from 37 to 40 °C (see Figs 4 and 5, curves *4*).

The study of the temperature effect (25—45 °C) on the conductivity (χ) of CTAB solutions revealed that the shape of the temperature dependences of χ for solutions with a concentrations of $1 \cdot 10^{-3}$ (Fig. 6, *a*) and $1.0 \cdot 10^{-4}$, $1.0 \cdot 10^{-7}$, and $1.0 \cdot 10^{-9}$ mol L^{-1} (Fig. 6, *b*) is opposite. The temperature dependences of χ for solutions with $1.0 \cdot 10^{-4}$, $1.0 \cdot 10^{-7}$, and $1.0 \cdot 10^{-9}$ mol L^{-1} are almost symbate.

For a solution with the concentration $1 \cdot 10^{-3}$ mol L^{-1} (see Fig. 6, *a*), the temperature increase from 25 to 30 °C

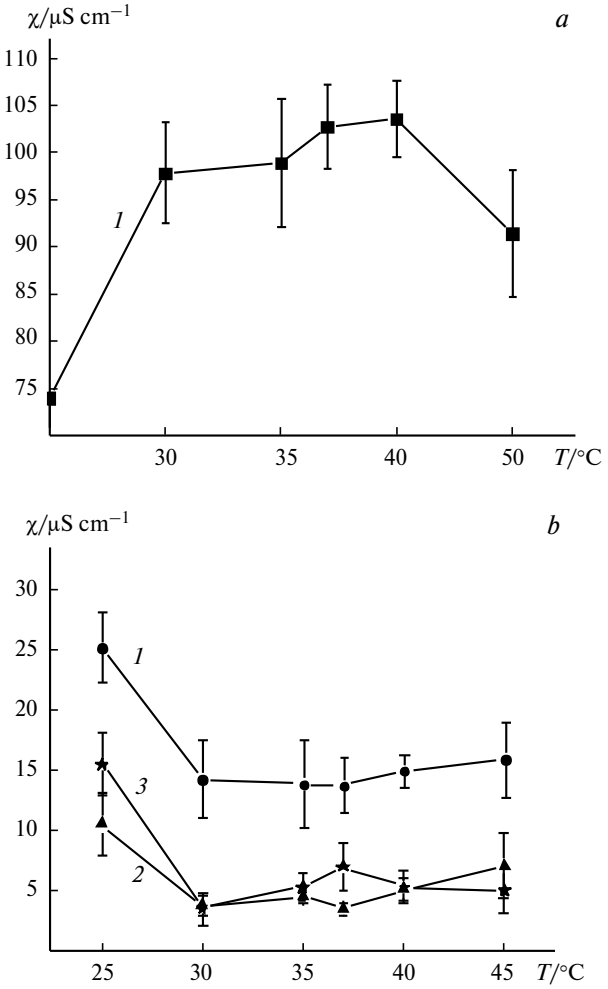

Fig. 6. *a*, Temperature dependence of the conductivity (χ) of a CTAB solution with the concentration $1 \cdot 10^{-3}$ mol L^{-1} (*1*). *b*, Temperature dependences of the conductivity (χ) of a CTAB solution with the concentrations $1.0 \cdot 10^{-4}$ (*1*), $1.0 \cdot 10^{-7}$ (*2*), and $1.0 \cdot 10^{-9}$ mol L^{-1} (*3*).

results in an increase in the conductivity of the solution by 30%, which is probably caused by an increase in the solubility of CTAB above the Krafft point, which leads to an increase in the number of monomeric ions of cetyltrimethylammonium, bromide ions, and CTAB molecules in solution, *i.e.*, an increase in the total number of charges in the solution bulk.[16] In the temperature range 30—45 °C, the conductivity of a CTAB solution with a concentration of $1 \cdot 10^{-3}$ mol L^{-1} changes insignificantly (see Fig. 6, *a*). The observed minor increase and decrease in χ with a maximum at 40 °C can be due to a change in the number and size of micelles and domains similarly to that shown earlier.[9] This means that at a concentration of $1 \cdot 10^{-3}$ mol L^{-1} the shape of the temperature dependence of the conductivity of solution is probably due to a change in the dynamic equilibrium between ions, molecules, micelles, and domains and their rearrangements

that occur with a change in the temperature of a CTAB solution.

An opposite pattern is observed for the temperature dependence of the conductivity (χ) of a CTAB solution with the concentration $1.0 \cdot 10^{-4}$ mol L^{-1}, *i.e.*, in the range of formation of domains in the solution: with the temperature increase from 25 to 30 °C, χ decreases remaining further nearly unchanged up to 45 °C (see Fig. 6, *b*, curve *1*). A similar shape of the temperature dependence at lower absolute values of χ was established for the dependences obtained for solutions with the concentrations $1.0 \cdot 10^{-7}$ and $1.0 \cdot 10^{-9}$ mol L^{-1}, *i.e.*, in the range of formation of nanoassociates (see Fig. 6, *b*, curves *2* and *3*).

We have earlier found that the change in the size and ζ potential of domains and, to a higher extent, of nanoassociates is responsible for the nonmonotonic character of the concentration dependences of the physicochemical properties of highly diluted solutions.[15] Tight correlations between changes in χ of the solutions and in the ζ potential of nanoassociates during their concentration rearrangements were also established.

A comparison of the temperature dependences of the ζ potential of domains and nanoassociates (see Fig. 5, curves *2*—*4*) and χ of solutions at concentrations of $1.0 \cdot 10^{-4}$, $1.0 \cdot 10^{-7}$, and $1.0 \cdot 10^{-9}$ mol L^{-1} (see Fig. 6, *b*, curves *1*—*3*) indicates that the temperature rearrangements of domains and nanoassociates, as well as their concentration rearrangements (see Fig. 2) accompanied by a change in the ζ potential, result in changes in the conductivity of dilute solutions of CTAB with temperature.

In solutions with the concentration $1.0 \cdot 10^{-4}$ mol L^{-1}, *i.e.*, an order of magnitude higher than the threshold concentration equal to $1.0 \cdot 10^{-5}$ mol L^{-1}, the ζ potential of domains changes with temperature from +25 to +2 mV with a minimum (+2 mV) at 30 °C (see Fig. 5, curve *2*). At concentration of $1.0 \cdot 10^{-7}$ and $1.0 \cdot 10^{-9}$ mol L^{-1}, which is several orders of magnitude lower than the threshold value, the ζ potential of nanoassociates changes with temperature from −10 to 0 mV with a minimum (0 mV) at 30 °C, whereas the dependences for solutions with a concentration of $1.0 \cdot 10^{-9}$ mol L^{-1} contain an additional maximum (−10 mV) at 37 °C (see Fig. 5, curves *3* and *4*). The exchange of the sign of the ζ potential of domains and nanoassociates is explained by the fact that the positive charge of the domain is determined by cetyltrimethylammonium cations in the domain composition, and the negative sign of the charge of nanoassociates is determined by quasi-crystalline structures of water that form a nanoassociate.[33]

Thus, the temperature dependence of the conductivity of CTAB solutions with concentrations of $1.0 \cdot 10^{-4}$, $1.0 \cdot 10^{-7}$, and $1.0 \cdot 10^{-9}$ mol L^{-1} correlates with the temperature dependence of the ζ potential of domains and nanoassociates formed at these concentrations of solutions. A minor but reliable increase in χ at 37 °C in a solution with the concentration $1.0 \cdot 10^{-9}$ mol L^{-1} (see Fig. 6, *b*, curve *3*) is consistent with an increase in nanoassociate size (see Fig. 4, curve *4*) and is explained by the formation of complicated space—time fractal structures responsible for the increase in the conductivity of a solution of low concentrations.[34,35]

It is known that the ESR spin probe method is one of informative methods of studying nanosized aggregates. When the probe is solubilized in nanosized structures, the change in the ESR spectrum makes it possible to estimate the degree of restriction of motion of the nitroxyl probe and to determine such important characteristics of aggregates as microviscosity, packing density, and degree of ordering of the structure in the zone of localization of a radical probe. TEMPO is often used as the latter.[36,37]

Taking into account low concentrations of CTAB solutions, we decided to study the self-organization and physicochemical properties of mixed CTAB/TEMPO solutions at the constant TEMPO concentration equal to $5.0 \cdot 10^{-4}$ mol L^{-1} and CTAB concentrations in a range of $1 \cdot 10^{-2}$—$1.0 \cdot 10^{-11}$ mol L^{-1} at 25 °C.

No particles were observed by DLS at 25 °C in a TEMPO solution, whereas the formation of particles in the CTAB concentration ranges $1 \cdot 10^{-2}$—$3.0 \cdot 10^{-6}$ mol L^{-1} (Fig. 7, *a*, *b*) and $3.0 \cdot 10^{-8}$—$3.0 \cdot 10^{-10}$ mol L^{-1} (see Fig. 7, *c*) was reliably observed in a mixed CTAB/TEMPO solution. No particles were observed in a mixed CTAB/TEMPO solution in a concentration range of $1.0 \cdot 10^{-6}$—$1.0 \cdot 10^{-7}$ mol L^{-1}.

The concentration dependences of the particle sizes in individual solutions of CTAB and mixed CTAB/TEMPO solutions are presented in Fig. 8. In the whole concentration range studied, the run of the concentration dependence $D = f(C)$ is similar for solutions of CTAB and solutions of CTAB/TEMPO, except for the CTAB concentration range $1.0 \cdot 10^{-6}$—$1.0 \cdot 10^{-7}$ mol L^{-1}, in which, probably, nanoassociates cannot bind to TEMPO.

In the range of formation of micelles and domains in a CTAB solution, *i.e.*, at the CTAB concentration equal to $1 \cdot 10^{-2}$—$1.0 \cdot 10^{-4}$ mol L^{-1}, the concentration dependence of the particle size in a mixed CTAB/TEMPO solution slightly differs from the concentration dependence of the size of domains formed in a CTAB solution (see Figs 7 and 8). In the range of formation of nanoassociates ($1.0 \cdot 10^{-8}$—$1.0 \cdot 10^{-9}$ mol L^{-1}), the size of particles formed in a mixed CTAB/TEMPO solution (see Fig. 8, curve *2*) significantly exceeds the size of nanoassociates in a CTAB solution (Fig. 8, curve *1*). The change in the particle size in a CTAB/TEMPO solution in the range of CTAB concentrations from $1.0 \cdot 10^{-8}$ to $3.0 \cdot 10^{-10}$ mol L^{-1} compared to a CTAB solution and the absence of particles in a range of CTAB concentrations of $1.0 \cdot 10^{-6}$—$1.0 \cdot 10^{-7}$ mol L^{-1} indicate the selective ability of the nanoassociates to bind with probe molecules to form mixed clusters CTAB/TEMPO.

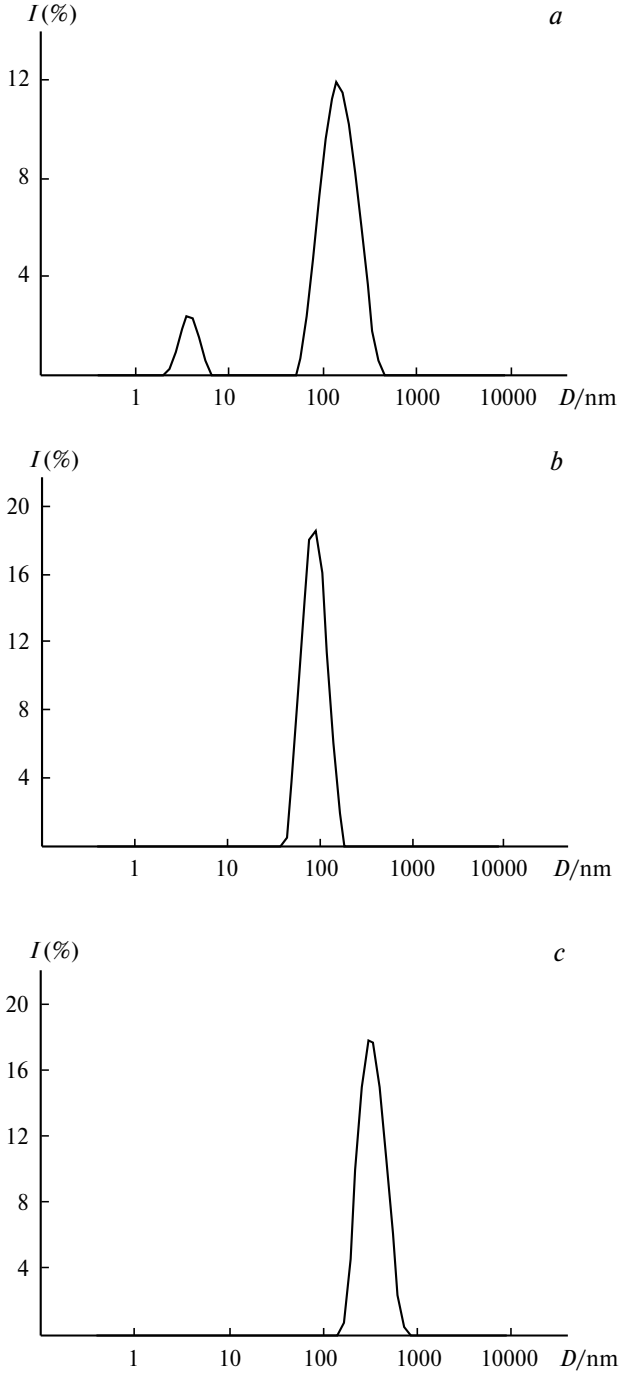

Fig. 7. Particle size distribution in a CTAB/TEMPO mixed system ($C_{TEMPO} = 5.0 \cdot 10^{-4}$ mol L^{-1}) at the CTAB concentrations $1 \cdot 10^{-3}$ (*a*), $1.0 \cdot 10^{-4}$ (*b*), and $1.0 \cdot 10^{-9}$ mol L^{-1} (*c*), 25 °C. *D* is the particle size, and *I* is the scattered light intensity.

The concentration dependences of the physicochemical properties (Fig. 9) of a mixed CTAB/TEMPO system in a concentration range of $1 \cdot 10^{-2}$—$1.0 \cdot 10^{-5}$ mol L^{-1}, which coincides with the concentration range of domain formation in CTAB solutions, differ slightly from similar dependences of the properties of individual CTAB

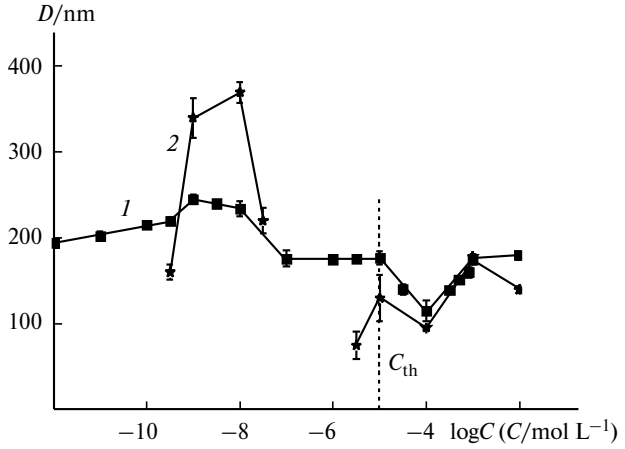

Fig. 8. Particle size (*D*) in aqueous solutions of CTAB (*1*) and CTAB/TEMPO (*2*) *vs* CTAB concentration, 25 °C. C_{th} is the threshold concentration.

(see Fig. 2). The dependences of the physicochemical properties (see Fig. 9) of a mixed CTAB/TEMPO system in a range of nanoassociate formation in CTAB solutions, *i.e.*, at concentrations of $1.0 \cdot 10^{-6}$—$1.0 \cdot 10^{-12}$ mol L^{-1}, are similar to the dependences of the nanoassociate sizes and properties of CTAB solutions and have a pronounced nonmonotonic character.

A specific feature of the CTAB/TEMPO system is the synergetic decrease in the surface tension (σ) from 52 mN m^{-1} at the CTAB concentration equal to $1.0 \cdot 10^{-9}$ mol L^{-1} and the TEMPO concentration equal to $5.0 \cdot 10^{-4}$ mol L^{-1} (see Fig. 9, curve *1*). In individual solutions of CTAB and TEMPO at these concentrations, the value of σ is equal to that of distilled water, being 71 mN m^{-1}. A similar synergetic decrease in σ is observed in a mixed system CTAB/4-sulfonatocalix[6]arene at a CTAB concentration of $1.0 \cdot 10^{-9}$ mol L^{-1}.[28] Solutions

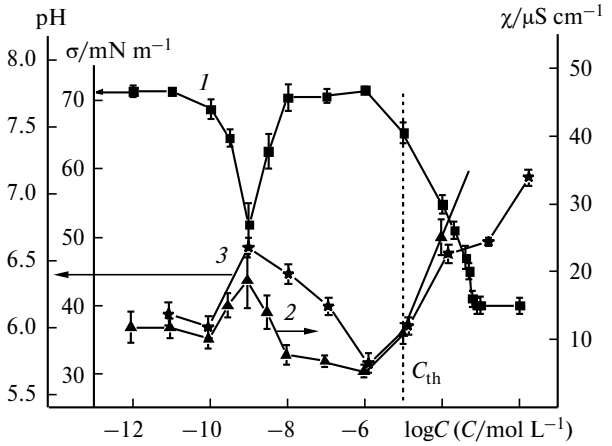

Fig. 9. Surface tension (σ) (*1*), conductivity (χ) (*2*), and pH (*3*) of a CTAB/TEMPO mixed system *vs* CTAB concentration; $C_{TEMPO} = 5.0 \cdot 10^{-4}$ mol L^{-1}, 25 °C. C_{th} is the threshold concentration.

of CTAB with a concentration of $1.0 \cdot 10^{-9}$ mol L^{-1} have a series of interesting properties (high catalytic activity in the hydrolysis of phosphorus acid ethers[38,39] and stimulating activity toward the bacterial growth[29]). These properties can be explained by the formation of nanoassociates with specific properties: the maximum size, possibly caused by the fractal spatial organization[34,35] of nanoassociates and, probably, a special ordering of quasi-crystalline structures of water forming nanoassociates at this concentration.[33]

Thus, the comparison of the concentration dependences of the particle sizes and physicochemical properties of CTAB/TEMPO solutions indicates the formation of mixed clusters in a CTAB concentration range of $1.0 \cdot 10^{-8}$—$1.0 \cdot 10^{-10}$ mol L^{-1}. The rearrangements of these clusters are accompanied by changes in the physicochemical properties of CTAB/TEMPO solutions.

It has been shown previously by the spin probe ESR method that at 25 °C the concentration dependence of the rotational diffusion correlation time (τ_{cor}) of the NO group of the probe bound to the CTAB structures formed in solution are nonlinear and symbate to the change in the concentration dependence of sizes of the domains and nanoassociates in a individual solution of CTAB.[15] In the present work, the temperature effect in the range 25—45 °C on τ_{cor} was studied by the ESR method in CTAB/TEMPO solutions at the TEMPO concentration equal to $5.0 \cdot 10^{-4}$ mol L^{-1} and CTAB concentrations of $1 \cdot 10^{-3}$, $1.0 \cdot 10^{-4}$, $1.0 \cdot 10^{-7}$, and $1.0 \cdot 10^{-9}$ mol L^{-1}. (Fig. 10). As can be seen from the data presented in Fig. 10, with the temperature increase the τ_{cor} value regularly decreases from 20 to 10 ps for all studied CTAB concentrations. Except for the CTAB concentration equal to $1.0 \cdot 10^{-7}$ mol L^{-1}, the temperature dependence of τ_{cor} has two to three plateaus between the inflection points in the linearized regions of the temperature dependences. One of them, in the range about 36—40 °C, is observed in the temperature dependences obtained for all concentrations. For a concentration of $1 \cdot 10^{-3}$ mol L^{-1}, at which micelles and domains are formed (see Fig. 10, *a*), the plateaus are

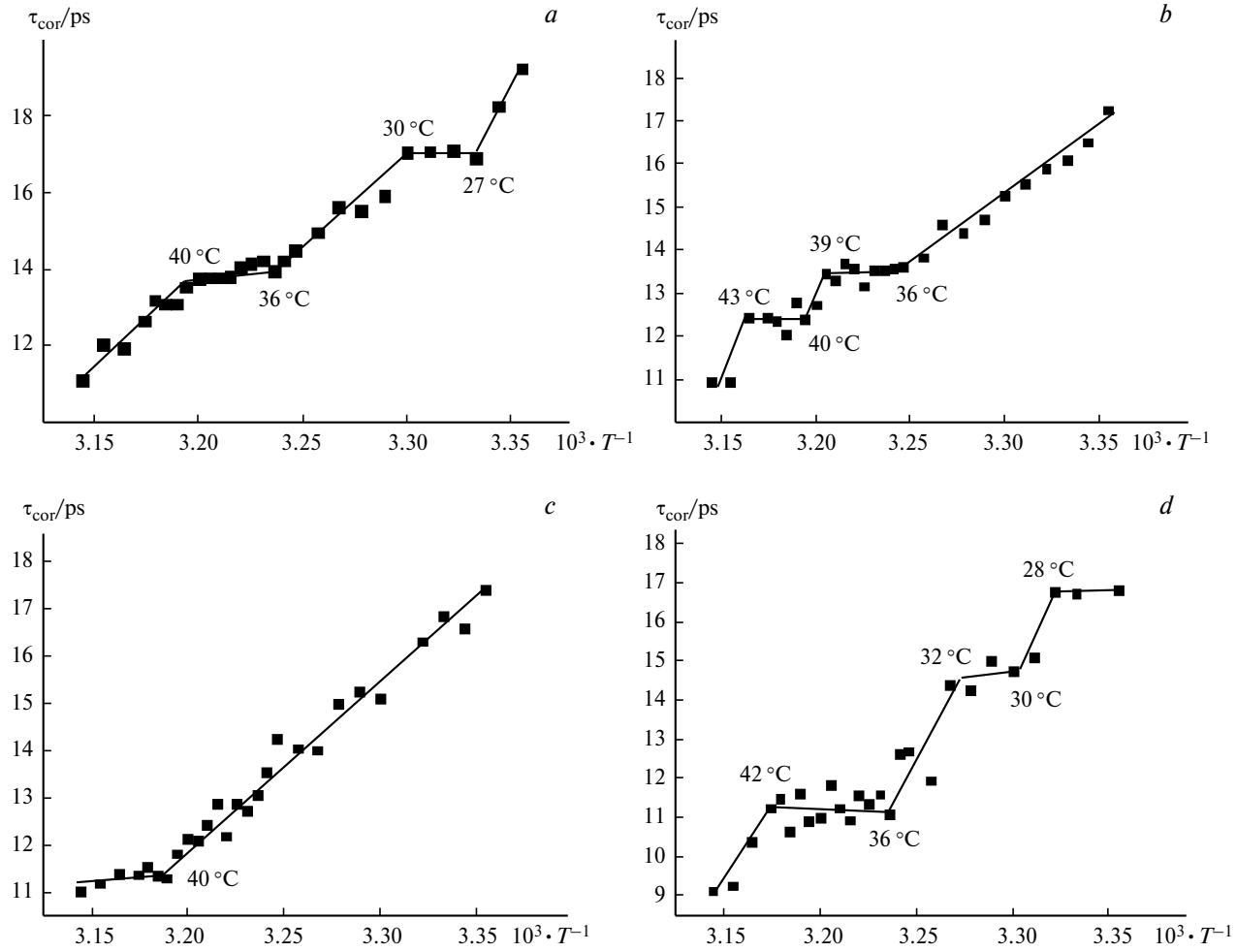

Fig. 10. Temperature dependences of the rotational diffusion correlation time (τ_{cor}) of the TEMPO probe in the Arrhenius coordinates at the CTAB concentrations in solutions equal to $1 \cdot 10^{-3}$ (*a*), $1.0 \cdot 10^{-4}$ (*b*), $1.0 \cdot 10^{-7}$ (*c*), and $1.0 \cdot 10^{-9}$ mol L^{-1} (*d*).

observed in the range 27—30 °C ($1 \cdot 10^{-3}$ mol L^{-1}) and 25—28, 30—32 °C ($1.0 \cdot 10^{-9}$ mol L^{-1}) in the range of nanoassociate formation (concentration $1.0 \cdot 10^{-9}$ mol L^{-1}) with extreme values of parameters (see Fig. 9, *d*), except for the plateaus in a range of 36—40 °C in the temperature dependence of τ_{cor}.

As shown above, with the increase in temperature of CTAB solutions, the nanostructures undergo rearrangements leading to extreme changes in their size and ζ potential (see Figs 4 and 5). A comparison of the temperature dependences of τ_{cor} obtained by the ESR method and the dependences of the particle size and ζ potential of domains and nanoassociates (see Fig. 4 and 5) obtained by DLS and electrophoresis indicates the identical temperature ranges containing plateaus in the τ_{cor} dependence and extreme changes in the size and ζ potential of domains and nanoassociates in CTAB solutions.

It is known that parameter τ_{cor} shows the characteristics of the nanoobject related to the probe, such as microviscosity and fluidity, and provides information about the structure.[36] Therefore, the pattern observed by the ESR method indicates structural rearrangements that occur in domains and nanoassociates with the temperature increase, which are probably accompanied by a change in the orientation of dipoles and mobility of water molecules forming nanoassociates and domains. This results in a change in their size and ζ potential (see Figs 4 and 5) and, as a consequence, the physicochemical properties of the solution (see Fig. 6).

Thus, it was revealed by a complex of physicochemical methods that dilute solutions ($1 \cdot 10^{-3}$, $1.0 \cdot 10^{-4}$, $1.0 \cdot 10^{-7}$ и $1.0 \cdot 10^{-9}$ mol L^{-1}) of surfactant cetyltrimethylammonium bromide in a temperature range of 25—45 °C are self-organized dispersed systems that undergo rearrangements specific for each studied concentration at each studied temperature. These specific rearrangements are observed as nonmonotonic temperature dependences of the parameters of the domains ($1 \cdot 10^{-3}$, $1.0 \cdot 10^{-4}$ mol L^{-1}) and nanoassociates ($1.0 \cdot 10^{-7}$, $1.0 \cdot 10^{-9}$ mol L^{-1}) as interrelated temperature dependences of the conductivity of solutions with extremes at 30, 37, and 40 °C. The ESR experiments revealed the temperature dependences of the rotational diffusion correlation time (τ_{cor}) of the TEMPO having a nonmonotonic decrease in τ_{cor} with the temperature increase from 25 to 45 °C and two to three plateaus. One of these plateaus in the temperature range about 36—40 °C is observed in the temperature dependences obtained for all studied concentrations.

The authors are grateful to E. G. Evtushenko (Department of Chemistry, M. V. Lomonosov Moscow State University) for help in NTA measurements.

This work was financially supported by the Russian Foundation for Basic research (Project No. 13-03-00002).

References

1. G. N. Zacepina, *Physical Properties and Water Structure*, Izd. Mos. Univ., Moscow, 1998, 136 pp.
2. Yu. P. Rassadkin, *Voda obyknovennaya i neobyknovennaya* [*Usual and Unusual Water*], Galereya STO, Moscow, 2008, 840 pp. (in Russian).
3. V. I. Lobyshev, *Ros. Khim. Zh.*, 2007, **51**, 107 [*Mendeleev Chem. J.* (*Engl. Transl.*), 2007, **51**].
4. R. Roy, W. A. Tiller, I. Bell, M. R. Hoover, *Mater. Res. Innovations Online*, 2005, **9**, 577.
5. D. Eisenberg, W. Kauzmann, *The Structure and Properties of Water*, Oxford Univ. Press, New York, 1969.
6. P. Ball, *H_2O: A Biography of Water*, Phoenix Press, London, 2000.
7. P. Ball, *Chem. Rev.*, 2008, **108**, 74.
8. V. Bardik, V. Gotsulskii, E. Pavlov, N. Malomuzh, D. Nerukh, I. Yanchuk, S. Lavoryk, *J. Mol. Liq.*, 2012, **176**, 60.
9. D. Hagmeyer, J. Ruesing, T. Fenske, H.-W. Klein, C. Schmuck, W. Schrader, M. E. M. da Piedade, M. Epple, *RSC Adv.*, 2012, **2**, 4690.
10. P. Bharmoria, H. Gupta, V. P. Mohandas, P. K. Ghosh, A. Kumar, *J. Phys. Chem. B*, 2012, **116**, 11712.
11. M. Sedlák, *J. Phys. Chem. B*, 2006, **110**, 4329.
12. M. Sedlák, *J. Phys. Chem. B*, 2006, **110**, 4339.
13. M. Sedlák, *J. Phys. Chem. B*, 2006, **110**, 13976.
14. M. Sedlák, D. Rak, *J. Phys. Chem. B*, 2013, **117**, 2495.
15. A. I. Konovalov, I. S. Ryzhkina, *Russ. Chem. Bull.* (*Int. Ed.*), 2014, **63**, 1 [*Izv. Akad. Nauk*, *Ser. Khim.*, 2014, 1].
16. K. Holmberg, B. Jonsson, B. Kronberg, B. Lindman, *Surfactants and Polymers in Aqueous Solutions*, 2nd ed., J. Wiley and Sons, 2003, 545 pp.
17. S. B. Savvin, R. K. Chernova, S. N. Shtykov, *Poverkhnostno-aktivnye veshchestva* [*Surfactants*], Nauka, Moscow, 1991, 251 pp. (in Russian).
18. V. V. Shkarin, M. Sh. Shafeev, *Dezinfektologiya: Rukovodstvo dlya studentov meditsinskikh vuzov i vrachei* [*Desinfectology: Manual for Students of Medical Higher Educational Institutions and Physicians*], Izd-vo Nizhegorod. Gos. Med. Akad., Nizhni Novgorod, 2003, 368 pp. (in Russian).
19. L. Chalmers, *Domestic and Industrial Chemical Specialties*, Leonard Hill, London, 1966.
20. E. F. Gale, E. Cundliffe, P. E. Reynolds, M. H. Richmond, M. Waring, *The Molecular Basis of Antibiotic Action*, Wiley-Intersci. Publ., J. Wiley and Sons, New York—London, 1972.
21. A. I. Rusanov, *Mitselloobrazovanie v rastvorakh poverkhnostno-aktivnykh veshchestv* [*Micelle Formation in Solutions of Surfactants*], Khimiya, St. Petersburg, 1992, 280 pp. (in Russian).
22. I. S. Ryzhkina, T. N. Pashirova, Ya. A. Filippova, *Zhidkie kristally i ikh prakticheskoe ispol´zovanie* [*Liquid Crystals and Their Practical Use*], 2003, **1**, 76 (in Russian).
23. I. S. Ryzhkina, T. N. Pashirova, Ya. A. Filippova, L. A. Kudryavtseva, A. P. Timosheva, V. P. Arkhipov, Z. Sh. Idiyatullin, E. V. Popova, A. R. Burilov, A. I. Konovalov, *Russ. Chem. Bull.* (*Int. Ed.*), 2004, **53**, 1520 [*Izv. Akad. Nauk*, *Ser. Khim.*, 2004, 1462].
24. E. P. Tishkova, L. A. Kudryavtseva, *Russ. Chem. Bull.* (*Int. Ed.*), 1996, **45**, 301 [*Izv. Akad. Nauk*, *Ser. Khim.*, 1996, 298].

25. V. G. Granik, *Russ. Chem. Bull.* (*Int. Ed.*), 2001, **50**, 1356 [*Izv. Akad. Nauk*, *Ser. Khim.*, 2001, 1291].
26. A. Dasgupta, P.K. Das, *J. Phys. Chem. B*, 2007, **111**, 8502.
27. A. Lattes, I. Rico-Lattes, E. Perez, V. I. Krutikov, B. Hamada, *Bull. Soc. Chim.*, 2007, **51**, 36.
28. I. S. Ryzhkina, Yu. V. Kiseleva, L. I. Murtazina, Yu. N. Valitova, S. E. Solov´eva, L. M. Pilishkina, A. I. Konovalov, *Russ. Chem. Bull.* (*Int. Ed.*), 2010, **59**, 1327 [*Izv. Akad. Nauk*, *Ser. Khim.*, 2010, 1297].
29. I. S. Ryzhkina, O. A. Mishina, A. P. Timosheva, Yu. V. Kiseleva, A. D. Voloshina, N. V. Kulik, A. I. Konovalov, *Dokl. Phys. Chem.* (*Engl. Transl.*), 2014, **459**, 166 [*Dokl. Akad. Nauk*, 2014, **459**, 51].
30. B. V. Deryagin, N. V. Churaev, F. D. Ovcharenko, *Voda v dispersnykh sistemakh* [*Water in Dispersed Systems*], Khimiya, Moscow, 1989, 288 pp. (in Russian).
31. S. M. Melnikov, V. G. Sergeyev, K. Yoshikawa, *J. Am. Chem. Soc.*, 1995, **117**, 2401.
32. *ASTM Standard E2834, 2012, Standard Guide for Measurement of Particle Size Distribution of Nanomaterials in Suspension by Nanoparticle Tracking Analysis (NTA)*, ASTM International, West Conshohocken (PA), 2012, DOI: 10.1520/E2834-12.
33. L. N. Gall, *Physical Principles of Functioning of a Live Organism Matter*, Izd. Politech. Univ., St. Petersburg, 2014.
34. I. V. Lunev, A. A. Khamzin, I. I. Popov, M. N. Ovchinnikov, I. S. Ryzhkina, O. M. Mishina, Yu. V. Kiseleva, A. I. Konovalov, *Dokl. Phys. Chem.* (*Engl. Transl.*), 2014, **455**, 56 [*Dokl. Akad. Nauk*, 2014, **455**, 656].
35. I. S. Ryzhkina, Yu. V. Kiseleva, A. P. Timosheva, R. A. Safiullin, M. K. Kadirov, Yu. N. Valitova, A. I. Konovalov, *Dokl. Phys. Chem.* (*Engl. Transl.*), 2013, **453**, 65 [*Dokl. Akad. Nauk*, 2012, **447**, 56].
36. A. N. Kuznetsov, *Metod spinovogo zonda* [*Spin Probe Method*], Nauka, Moscow, 1976 (in Russian).
37. A. I. Litvinov, V. I. Morozov, M. K. Kadirov, *Vestn. KTU* [*Bulletin of Kazan Technical University*], 2012, **11**, 28 (in Russian).
38. I. S. Ryzhkina, Yu. V. Kiseleva, A. I. Konovalov, *Abstr. of 6th Intern. Symp. "Supramolecular Systems in Chemistry and Biology" (Strasbourg, France, September 5—8, 2012)*, Strasbourg, 106.
39. Yu. V. Kiseleva, I. S. Ryzhkina, A. I. Konovalov, *Abstr. of 8th Annu. Conf. on the Physics, Chemistry and Biology of Water (Borovets, Bulgaria, October 22—25, 2013)*, Borovets; www.waterconf.org/site/YuliaKiseleva_abstract.pdf.

Received December 26, 2014;
in revised form January 23, 2015